

# Experimental Investigation of Compressible Nozzle Flow

Trae Nelson<sup>1</sup> | Zakary Steenhoek<sup>1</sup> | Justin Ritzenthaler<sup>1</sup> | Colin McArthur<sup>1</sup> | Nicolas Nelson<sup>1</sup>

*Arizona State University, Tempe, AZ, 85288, United States*

The purpose of this experiment was to investigate various parameters of compressible nozzle flow using a converging-diverging nozzle. A brief overview of the procedure of this experiment goes as follows. First, to prepare, ambient pressure and temperature were recorded along with their respective uncertainties. Next, thermometers were placed in dedicated locations before and after the nozzle to measure the inlet and outlet temperatures. Other important information such as nozzle diameter at each station and mass-flow meter corrections were also recorded. After preparation, the testing phase began. Several test runs were performed with the outlet gauge pressure fixed at 50kPa and the inlet pressure was set to 100, 200, 300, 400, and 450 kPa. For each run, the pressures were checked to verify they were correct and steady. Then, the rotameter, the inlet and outlet thermometers, and the pressure gauges at all intermediate stations were read and their values were recorded. The test phase was then repeated, with the inlet gauge pressure fixed at 450 kPa and the outlet pressure set to 50, 100, 200, 300, and 400 kPa. The results of this experiment showed clear trends that align with the known behavior of compressible flow through a converging-diverging nozzle. When the pressure ratio between the inlet and outlet was low, the flow stayed subsonic throughout the entire nozzle. When the pressure ratio between the inlet and outlet was high, the flow became choked at the throat with a Mach number of 1. This produced a normal shock in the diverging section. The normal shock moved down the section as the pressure ratio increased. The mass flow rate remained constant when the flow became choked when the inlet pressure was fixed, but it increased linearly when outlet pressure was fixed, and inlet pressure varied. The forces on the nozzle were found to have increased as the differences in pressure increased. Finally, Bernoulli's equation was shown to break down when used on the highspeed, compressible flows produced in this experiment, highlighting its invalidity at high Mach numbers. This experiment provided insights into how pressure, density, velocity, and temperature interact under high-speed, compressible flows, supporting the core principles of isentropic flow and shock dynamics, and illustrated the importance of understanding these complex flow dynamics when designing nozzles for real-world applications such as aerospace and industrial use.

## I. Nomenclature

A	=	Nozzle area ( $m^2$ )
a	=	Sound speed ( $m/s$ )
E	=	Energy ( $J$ )
e	=	Specific internal energy ( $J/kg$ )
F	=	Force ( $N$ )
g	=	Gravitational acceleration ( $m/s^2$ )
h	=	Specific enthalpy ( $J/kg$ )
h	=	Vertical height ( $m$ )
M	=	Molecular mass ( $kg/mol$ )
$M_f$	=	Mach number of flow
$M_s$	=	Shock Mach number
m	=	Mass ( $kg$ )
$\dot{m}$	=	Mass rate w.r.t. time ( $kg/s$ )

---

<sup>1</sup> Student, Arizona State University

$n$	= Numerical subscript; denotes any nomenclature at a specific location
$\hat{n}$	= Normal unit vector
$p$	= Pressure (kPa)
$p_0$	= Stagnation pressure (kPa)
$\dot{q}$	= Heat rate per unit mass w.r.t. time ( $J/kg \cdot s$ )
$\mathcal{R}$	= Universal gas constant ( $J/mol \cdot K$ )
$R$	= Specific gas constant ( $J/kg \cdot K$ )
$S$	= Control volume surface ( $m^2$ )
$T$	= Temperature (K)
$T_0$	= Stagnation temperature (K)
$t$	= Time (s)
$u$	= Velocity of flow (m/s)
$V$	= Conservation integral equations flow velocity (m/s)
$\mathcal{V}$	= Control volume ( $m^3$ )
$x$	= arbitrary variable used as a placeholder for future variables
$y$	= arbitrary variable used as a placeholder for future variables
$\gamma$	= Specific heat ratio
$\delta$	= Uncertainty
$\rho_0$	= Stagnation density ( $kg/m^3$ )
$\rho$	= Density ( $kg/m^3$ )
$\Sigma$	= Summation
$\partial$	= Partial derivative
$*$	= Denotes sonic condition for any nomenclature

## II. Introduction

In this experiment, analysis is performed on a convergent-divergent nozzle (C-D nozzle). C-D nozzles are sometimes referred to as *de Laval nozzles*, after Carl G. P. de Laval. Laval first used a C-D nozzle configuration in steam turbines during the late nineteenth century. C-D nozzles are utilized to accelerate subsonic flow to supersonic speeds or decelerate supersonic flow to subsonic speeds. In this experiment, the C-D nozzle is used to accelerate the flow to supersonic speeds so its properties can be analyzed. A C-D nozzle consists of a converging section, a throat, and a diverging section. The converging section is fed an inlet flow from a reservoir. This reservoir has a pressure denoted by  $p_0$ . As the flow moves through the converging section at subsonic speeds, it is accelerated until it reaches Mach 1 at the throat where the area is at its smallest. Equation 1 below shows the area-velocity relation (derived from the conservation of momentum).

$$\frac{dA}{A} = (M_f^2 - 1) \cdot \frac{du}{u} \quad (1)$$

Plugging in a value of  $M_f = 1$  into this equation shows that for the Mach number to equal 1, the area must be at its minimum [1]. This is why the Mach number at the throat is equal to 1. After the flow reaches sonic speed at the throat, the diverging section continues to accelerate the flow. Figure 1 shows the schematic of a C-D nozzle like the one used in this experiment.

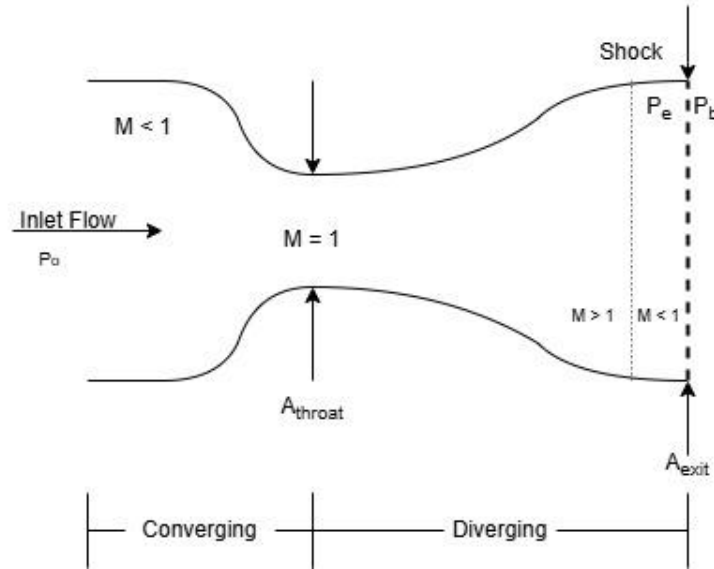


**Fig. 1. Experimental schematic of a converging-diverging nozzle.**

In aerodynamics, a flow can be assumed to be incompressible if the flow speed is less than a Mach number of 0.3. When flow is assumed to be incompressible, it's assumed that its density is constant throughout the flow [2]. In the case of a C-D nozzle, this assumption is no longer valid, and the flow must be considered compressible due to the high speeds near and after the throat. After the flow reaches the throat, the diverging section causes the gas to expand and accelerate, showing changes in density. Thus, the flow is compressible.

Equation 1 shows the relationship between area, Mach number, and velocity as area and velocity change. There are two specific cases investigated in this experiment, one for subsonic flow and one for supersonic flow. If the flow is subsonic the velocity of the flow will decrease as it passes through a section of diverging area and increase as it passes through a section of converging area. If the flow is supersonic the velocity will increase as it passes through a section of diverging area and increase as it passes through a section of converging area.

If the flow reaches a Mach number greater than 1, it is possible for a shock to form in the nozzle. Because shocks are non-isentropic, the isentropic relations cannot be used across them, but they can be used between any two points in the nozzle not separated by a shock. For a shock to form in the nozzle, the exit pressure in the divergent section must be less than the ambient pressure of the atmosphere the gas is being expelled into. Shocks will occur at different locations depending on the values of these pressures.

An important concept in C-D nozzles is choked flow. Choked flow occurs when the Mach number at the throat is equal to one. The ratio of exit pressure over inlet pressure can be used to determine if the flow is choked or not. When the flow is choked, the maximum airflow limit (mass flow rate) through the converging section is achieved. The properties of total pressure and temperature are also constant in the converging section if the flow is choked. The flow properties will remain constant even if the exit pressure continues to decrease [3].

### III. Procedures

The following is a detailed description of the laboratory equipment used, and the procedures followed for experimental data collection and data processing used to carry out this experiment.

#### A. Experimental Equipment

The experimental equipment used includes primarily the nozzle-flow test rig owned by Arizona State University and operated in the aerospace engineering lab space, which consists of multiple sub-components. An absolute pressure transducer and a digital thermocouple are used as well.

##### 1. Nozzle-flow test setup

The main piece of equipment used is the nozzle-flow setup, shown in Fig. 2, which allows the study of compressible flow under controlled conditions. The inlet is connected to a pressurized air supply, where the influx of air is controlled with an adjustable valve and monitored using the inlet pressure gauge. The inlet air temperature is

measured with a traditional thermometer before passing through the converging-diverging nozzle regime. The nozzle is tapped and connected to pressure gauges at eight different locations to obtain pressure readings as the air flows through the test rig. Note that these pressure readings are in gauge pressure rather than absolute pressure. The exiting air temperature is measured once again with a thermometer before passing through a mass-flow rotameter, which measures the mass flow rate through the system. A second adjustable valve is located at the exit, just before the mass-flow rotameter, allowing the back pressure to be varied and measured. The test rig also includes a correction factor chart, which accounts for the effects of ambient temperature and pressure on the mass flow measurements.

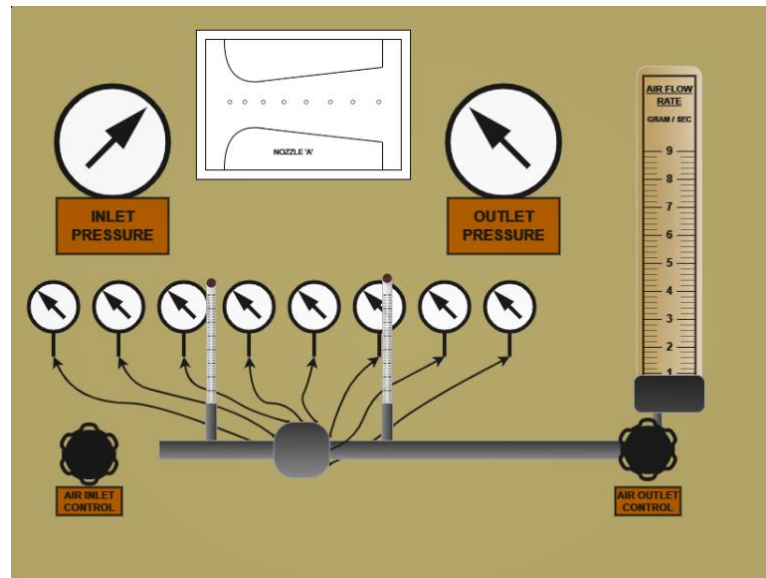


**Fig. 2. Nozzle-flow test setup. Note the inlet and outlet valves, eight pressure taps, two thermometers, and mass-flow rotameter.**

### 2. Absolute pressure transducer

An absolute pressure transducer was used to measure the ambient static pressure in the laboratory. This device measures absolute pressure, or the pressure relative to a perfect vacuum, and writes a proportional output in volts. This is converted automatically and displayed in kilopascals.

### 3. Digital thermocouple

The digital thermocouple was used to measure the ambient static temperature in the laboratory. This device measures the temperature difference between two metal plates and writes a proportional output in volts, which is automatically converted and displayed in degrees Celsius.

## B. Data Collection

The data collection procedure involves recording the ambient conditions in the laboratory, configuring the components of the testing setup, and collecting flow data under varying the inlet and outlet pressure conditions. The collected data includes both the inlet and outlet pressures, the pressures at all 8 locations through the nozzle, the temperature of the flow before and after passing through the nozzle, and the mass flow rate. Collected data is then processed using fundamental compressible flow equations and analyzed to extract meaningful results.

### 1. Measuring ambient conditions & equipment setup

First, the ambient pressure and temperature conditions are measured using the pressure transducer and digital thermocouple, respectively. These measurements are used as reference values for determining the correct correction factor that should be applied to the mass-flow rotameter readings. These measurements also allow the ambient air density and sound speed to be computed for later use in the data processing procedure.

To set up the nozzle-flow test rig, it's firstly ensured that the inlet valve is shut before connecting the high-pressure air supply line. The thermometers are placed in dedicated locations fore and aft of the nozzle to measure the temperature at these locations. The correction factor is found in the machine chart before beginning any flow testing.

## 2. Changing inlet pressure

Once setup is complete, the inlet valve is opened to allow flow through the test rig. The first phase of testing aims to determine the effects of varying the pressure at the inlet while keeping the outlet pressure, or back pressure, constant. The inlet and outlet valves are adjusted to meet the first test condition, where the inlet pressure is set at 100 kPa and the outlet pressure is set at 50 kPa. Note that changing the pressure at one side often influences the other, so care must be taken to ensure the pressures at both sides are correct. After verifying that the pressures are correct and holding steady, the pressure readings at each of the 8 locations through the nozzle regime are recorded. The temperature readings from both thermometers are recorded, as well as the mass-flow rotameter reading.

This same procedure is performed four more times for different magnitudes of pressure at the inlet. The outlet pressure is held constant through all these iterations at 50 kPa. The inlet pressure is increased from 100 kPa to 200 kPa, 300 kPa, 400 kPa, and finally 450 kPa. Through each of these pressure conditions, the same care is taken in adjusting the inlet and outlet valves to ensure accuracy and consistency through the data collection process. This phase of testing should yield 8 pressure readings, 2 temperature readings, and a mass rate for 5 magnitudes of inlet pressure at a constant back pressure.

## 3. Changing outlet pressure

The next phase of data collection aims to determine the effects of varying the pressure at the outlet while keeping the inlet pressure constant. The first pressure condition for this phase is the same as the final pressure condition for the last phase, i.e. 450 kPa at the inlet and 50 kPa at the outlet, so no changes to the inlet or outlet valves are required. Ensuring that the pressures are still accurate and steady, the same pressure, temperature, and mass rate values are recorded.

Like the previous phase, data is collected this time at four magnitudes of back pressure with constant inlet pressure. The outlet pressure ranges from the initial 50 kPa to 100 kPa, 200 kPa, 300 kPa, and finally 400 kPa. Once again, noting that care must be taken to ensure accurate and steady pressures before taking data measurements. This phase of testing should also yield 8 pressure readings, 2 temperature readings, and a mass rate for the 5 magnitudes of outlet pressure at a constant inlet pressure. The final data set should contain these readings for a total of 10 different pressure differentials, where 2 cases have the same differential pressure.

# C. Data Processing

## 1. Fundamental derivations

The governing equation for air density is the fundamental ideal gas law, which relates pressure, volume, temperature, matter, and the universal gas constant. This equation can be rearranged by expanding the term representing matter into mass over molar mass,  $m/M$ , defining the specific gas constant  $R$  as  $R/M$ , dividing by volume, and introducing density as  $m/V$ , seen below. This yields Eq. (2) for density:

$$pV = nRT \rightarrow p = \frac{nR}{V} \cdot T \rightarrow p = \frac{m}{V} \cdot \frac{R}{M} \cdot T \rightarrow p = \rho RT$$

$$\rho = \frac{p}{RT} \quad (2)$$

Where the specific gas constant is known for air,  $R_{air} = R = 287 \text{ J/kg} \cdot \text{K}$ . The uncertainty associated with this measurement is found using the Gaussian error propagation formula, the partial derivatives of Eq. (2) w.r.t.  $p$  and  $T$ , and the known machine errors,  $\delta p$  and  $\delta T$ , yielding Eq. (3) for the density uncertainty:

$$\delta y = \sqrt{\sum_i^n \left( \frac{\partial y_i}{\partial x_i} \cdot \delta x_i \right)^2} \rightarrow \delta \rho = \sqrt{\left( \frac{\partial \rho}{\partial p} \cdot \delta p \right)^2 + \left( \frac{\partial \rho}{\partial T} \cdot \delta T \right)^2}$$

$$\delta \rho = \sqrt{\left( \frac{1}{RT} \cdot \delta p \right)^2 + \left( \frac{p}{RT^2} \cdot \delta T \right)^2} \quad (3)$$

Conservation of mass is one of the fundamental governing equations in compressible flow analysis. It can be assumed that the flow through the converging-diverging nozzle regime is steady and quasi-one-dimensional. Mass rate is a constant with respect to time, and fluid parameters change as a function of a single positional coordinate

through the testing setup. The flow regime is also assumed to be adiabatic; no heat or work energy is gained or lost by the fluid. Then, the flow at any point along the single dimension is assumed to be constant across the entire cross-sectional area, greatly simplifying the general mass conservation equation as seen below:

$$\begin{aligned} \iiint_S \rho V \cdot dS &= -\frac{\partial}{\partial t} \iiint_V \rho \, dV \\ \int_{A_1} \rho(\vec{V}_1 \cdot \hat{n}_1) \, dA_1 + \int_{A_2} \rho(\vec{V}_2 \cdot \hat{n}_2) \, dA_2 &= 0 \\ \int_{A_1} \rho(\vec{V}_1 \cdot \hat{n}_1) \, dA_1 &= \int_{A_2} \rho(\vec{V}_2 \cdot \hat{n}_2) \, dA_2 \\ \dot{m} &= \rho_1 u_1 A_1 = \rho_2 u_2 A_2 \end{aligned} \quad (4)$$

This yields the familiar equation for mass conservation, Eq. (4), which holds at any location in the test rig. Conservation of momentum is another fundamental governing equation in compressible flow analysis. The adiabatic assumption means the only force is applied to the nozzle by the flow, so under the assumptions listed above, it is simplified from the general integral form to Eq. (5):

$$\begin{aligned} \iint_S (\rho V \cdot dS) V + \iiint_V \frac{\partial(\rho V)}{\partial t} \, dV &= \iiint_V \rho f \, dV - \iint_S p \, dS \\ \int_{A_1} \rho \vec{V}_1 (\vec{V}_1 \cdot \hat{n}_1) \, dA_1 + \int_{A_2} \rho \vec{V}_2 (\vec{V}_2 \cdot \hat{n}_2) \, dA_2 + \int_{A_1} p_1 \hat{n}_1 \, dA_1 + \int_{A_2} p_2 \hat{n}_2 \, dA_2 &= \sum \vec{F}_{ext} \\ -\rho_1 u_1^2 A_1 + \rho_2 u_2^2 A_2 - p_1 A_1 + p_2 A_2 &= F_{ext} \end{aligned} \quad (5)$$

The final governing conservation equation is the conservation of energy. Still under the same assumptions, the general integral form simplifies to Eq. (6) after dividing by Eq. (4) and applying the enthalpy equivalence, where  $h = e + p/\rho$ :

$$\begin{aligned} \iiint_V \dot{q} \rho \, dV - \iint_S p V \cdot dS + \iiint_V \rho (f \cdot V) \, dV &= \iiint_V \frac{\partial}{\partial t} \left[ \rho \left( e + \frac{V^2}{2} \right) \right] \, dV + \iint_S \rho \left( e + \frac{V^2}{2} \right) V \cdot dS \\ p_1 u_1 A_1 + \rho_1 u_1 A_1 \left( e_1 + \frac{u_1^2}{2} \right) &= p_2 u_2 A_2 + \rho_2 u_2 A_2 \left( e_2 + \frac{u_2^2}{2} \right) \\ \frac{p_1}{\rho_1} + e_1 + \frac{u_1^2}{2} &= \frac{p_2}{\rho_2} + e_2 + \frac{u_2^2}{2} \\ h_1 + \frac{u_1^2}{2} &= h_2 + \frac{u_2^2}{2} \end{aligned} \quad (6)$$

An alternate expression for energy conservation is well-known as the Bernoulli equation. The expression equates total fluid energy at any point to the sum of the pressure, kinetic, and gravitational energies at that point, which is a constant in the flow regime. It is seen more in low-speed fluid mechanics, as it is rooted in the assumption that the fluid density is a constant. This assumption progressively degrades as the Mach number increases; the standard accepted Mach number ceiling for an incompressible flow regime is  $M = 0.3$ , well below the *typical* range for most nozzle flows. The contributing energy components per unit mass are:

$$\begin{aligned} E_{pressure} &= \frac{p}{\rho} \\ E_{kinetic} &= \frac{V^2}{2} \\ E_{grav} &= gh \end{aligned}$$

Note that since air has a low relative density and the test rig is horizontal, the gravitational term will be neglected. Knowing that the Bernoulli equation is not an accurate representation of energy in compressible flow, the magnitude of inaccuracy can be measured by evaluating Eq. (7.1) at two stations where all quantities are already known. Then Eq. (7.2) can be used to determine the percentage difference between the total energy prediction at these two points. As Eq. (7.1) is an equivalency, a non-negligible percentage difference between two stations verifies that density changes must be considered at that flow condition.

$$\frac{p_1}{\rho_1} + \frac{V_1^2}{2} = \frac{p_2}{\rho_2} + \frac{V_2^2}{2} \quad (7.1)$$

$$\% \text{ Difference: } \frac{|\text{LHS} - \text{RHS}|}{\left( \frac{\text{LHS} + \text{RHS}}{2} \right)} \cdot 100 \quad (7.2)$$

Note that Eq. (7.2) is simply an application of the standard error percentage equation. In high-speed analysis, the sound speed equation and Mach number definition are critical parameters for the governing thermodynamic relations used in nozzle flows. These are well-defined as Eq. (8) and Eq. (9):

$$a = \sqrt{\gamma RT} \quad (8)$$

$$M = \frac{u}{a} \quad (9)$$

The thermodynamic relations mentioned earlier are founded upon the assumption that the changes in flow condition are isentropic, or reversible without energy loss. The isentropic process only exists in theory, but like many assumptions, this approximates entropy generation to negligible amounts. Then the isentropic relations, which relate the stagnation properties to any local condition, can be used. These relations vary only as a function of the local Mach number and known thermodynamic constants. The isentropic relations exist for flow parameters as Eqs. (10.1-10.3):

$$\frac{T_0}{T} = \left[ 1 + \frac{\gamma - 1}{2} M^2 \right] \quad (10.1)$$

$$\frac{p_0}{p} = \left[ 1 + \frac{\gamma - 1}{2} M^2 \right]^{\frac{\gamma}{\gamma - 1}} \quad (10.2)$$

$$\frac{\rho_0}{\rho} = \left[ 1 + \frac{\gamma - 1}{2} M^2 \right]^{\frac{1}{\gamma - 1}} \quad (10.3)$$

Where the subscription '0' denotes the stagnation, or total flow property, and  $\gamma$  is the ratio of specific heats. For air, this ratio is  $\gamma_{air} = 1.4$ . These relations describe the amount of energy associated with moving at some Mach number relative to the total fluid energy, measured as if the fluid was reduced to stagnation in an isentropic process. From these, two governing equations for flow through converging and diverging nozzles are found, known as the area-velocity relation and the area-Mach relation. The former is derived from Eqs. (4-5), where the isentropic assumption extends to say that, for any  $dp$ , there exists a corresponding isentropic  $d\rho$ . This can be expressed in terms of sound speed, thus:

$$\begin{aligned} d(\rho u A) &= d(\dot{m}) \rightarrow \frac{d\rho}{\rho} + \frac{du}{u} + \frac{dA}{A} = 0 \\ dp &= -\rho u du \rightarrow \frac{dp}{\rho} = -u du = \frac{dp}{d\rho} \cdot \frac{d\rho}{\rho}, \quad \text{where} \quad \frac{dp}{d\rho} = \left( \frac{\partial p}{\partial \rho} \right)_s = a^2 \\ a^2 \cdot \frac{d\rho}{\rho} &= -u du \rightarrow \frac{d\rho}{\rho} = -\frac{u^2 du}{a^2 u} = -M^2 \frac{du}{u} \\ \frac{dA}{A} &= (M^2 - 1) \frac{du}{u} \end{aligned} \quad (11)$$

Equation (11) relates changes in area, changes in flow velocity, and the Mach number. It states that acceleration from a subsonic to a supersonic Mach number requires convergence *and* divergence. Also, the flow through the most restrictive cross-sectional area, known as the throat, must be exactly sonic. The other equation that governs compressible nozzle flow is Eq. (12), known as the area-Mach relation. It derives from Eq. (4) between any condition and the sonic reference condition, as well as the isentropic density and Mach relations:

$$\begin{aligned} \dot{m} &= \rho^* u^* A^* = \rho u A \rightarrow \frac{A}{A^*} = \frac{\rho^* u^*}{\rho u} = \frac{\rho^* \rho_0 a^*}{\rho_0 \rho u}; \quad u^* = a^* \text{ for } M^* = 1 \\ \frac{\rho_0}{\rho} &= \left[ 1 + \frac{\gamma - 1}{2} M^2 \right]^{\frac{1}{\gamma - 1}} \rightarrow \frac{\rho_0}{\rho^*} = \left[ \frac{\gamma + 1}{2} \right]^{\frac{1}{\gamma - 1}}; \quad M^{*2} = \frac{(\gamma + 1) M^2}{2 + (\gamma - 1) M^2} \\ \frac{A}{A^*} &= \frac{1}{M} \left[ \frac{2}{\gamma + 1} \cdot \left( 1 + \frac{\gamma - 1}{2} M^2 \right) \right]^{\frac{\gamma + 1}{2(\gamma - 1)}} \end{aligned} \quad (12)$$

Equation (12) dictates the throat area required for a choked flow to accelerate to a Mach number, assuming the back pressure allows. Determining the theoretical shock location in the post-throat regime requires a final set of relations to relate the pre-shock and post-shock properties, known as the normal shock relations. These exist for pressure, density, temperature, and Mach number, defined as:

$$\frac{p_2}{p_1} = 1 + \frac{2\gamma}{\gamma + 1} (M_1^2 - 1) \quad (13.1)$$

$$\frac{\rho_2}{\rho_1} = \frac{(\gamma + 1) M_1^2}{2 + (\gamma - 1) M_1^2} \quad (13.2)$$

$$M_2^2 = \frac{1 + \frac{\gamma - 1}{2} M_1^2}{\gamma M_1^2 - \frac{\gamma - 1}{2}} \quad (13.3)$$

$$\frac{T_2}{T_1} = \frac{p_2}{p_1} \cdot \frac{\rho_1}{\rho_2} \quad (13.4)$$

The shock theoretical shock location in the nozzle can then be estimated by applying a combination of the relations above. By assuming a shock exists and linking together appropriate pressure ratios through the nozzle regime, where the subscript '0' denotes stagnation pressure and a prime denotes the local static pressure as required by normal shock relations:

$$\frac{p_{0_8}}{p_{0_1}} = \frac{p_{0_8}}{p_{8'}} \cdot \frac{p_{8'}}{p_{1'}} \cdot \frac{p_{1'}}{p_{0_1}}$$

An expression for the stagnation pressure ratio is obtained as a function of known pressure relations. Both the static and stagnation pressures change over a shock, so correctly daisy-chaining these ratios and substituting the relevant equivalencies discussed above simplifies the ratio chain to a function of just the shock Mach number, thermodynamic constants, and the stagnation pressure ratio:

$$\frac{p_{0_8}}{p_{0_1}} = \left[ \frac{(\gamma + 1)M_s^2}{(\gamma - 1)M_s^2 + 2} \right] \cdot \left[ \frac{\gamma + 1}{2\gamma M_s^2 - (\gamma - 1)} \right] \quad (14)$$

Which is the last of the relations needed for analyzing the collected data. The procedure for applying these relations and equations to the data is discussed next.

## 2. Implementation and presentation

After following the laboratory procedure to collect data, MATLAB is used to implement data processing and presentation. The raw data is first imported, sorted, and named appropriately. Ensuring to apply the correct mass rate correction factor, convert temperature readings from degrees Celsius to Kelvin, and convert the gauge pressure readings to absolute pressure. The position and diameter of each of the pressure taps are known data from the test rig, which allows the tap areas, including the throat area, to be computed. The known thermodynamic constants for air are also set.

For each of the 10 pressure conditions at which data was collected, density and uncertainty are found directly from Eqs. (2-3) since temperature and pressure are known. Mass rate is known from collected data, so flow velocity can be found from Eq. (4). The ambient temperature is known, thus Eq. (8) is used to find the speed of sound and used in Eq. (9) with the computed velocity to determine the isentropic Mach number distribution through the nozzle. Then Eq. (10.2) can be used to find stagnation pressure at both the first and the last station, which prescribes the total pressure ratio across the nozzle. Recognize that this ratio solves Eq. (14) for the shock Mach number if a shock is present.

Before moving on to predicting the shock location, the force of the fluid on the nozzle for each case can be found from Eq. (5). Knowing the pressure, density, and fluid velocity at the first and last station means the Bernoulli equation applicability test discussed above can be done as well. Equations (7.1-7.2) allow analytical data analysis to support or dispute the traditional incompressible cutoff Mach of ~0.3.

Continuing the effort to determine the theoretical shock location, Eq. (14) is attempted for all tests. In MATLAB, solving Eq. (14) must be done numerically, as it represents a combined nonlinear system. This is done using the built-in function 'fsolve()' and providing an initial guess. A shock in the nozzle does not form in all 10 tests. This means shock existence must still be verified. For a shock to form, the nozzle throat must be choked, and the back pressure must permit the isentropic expansion solution. It's checked if any of the conditions aren't met. In MATLAB, this is clearly indicated in the solutions to Eq. (14) – the numerical method will return a shock Mach less than one, which is known to be impossible. The raw data can also be examined to get a rough idea of which tests saw normal shock formation. Instantaneous large pressure increases, or Mach decreases are indicative of a normal shock jump. There's also the known critical pressure ratio for air that can be compared to the total pressure ratios for each test.

After Eq. (14) solves the theoretical shock Mach number, Eq. (12) is applied to determine the area ratio for which this shock Mach occurs. Knowing the nozzle throat area then solves this ratio for the area at which the theoretical shock occurs. This shock area is compared to the known nozzle geometry, and the corresponding station location is solved. The processed data is stored, and digital plots are generated to extract meaningful results to support the relevant discussion of the experimental trends.



#### IV. Results

The results below were obtained by varying the inlet and outlet pressure of the nozzle test rig, recording the pressure at eight pressure taps varied across the nozzle. The mass flow rate and temperature were also recorded through the nozzle. After completing the data analysis of the measurements, the following experimental results were obtained.

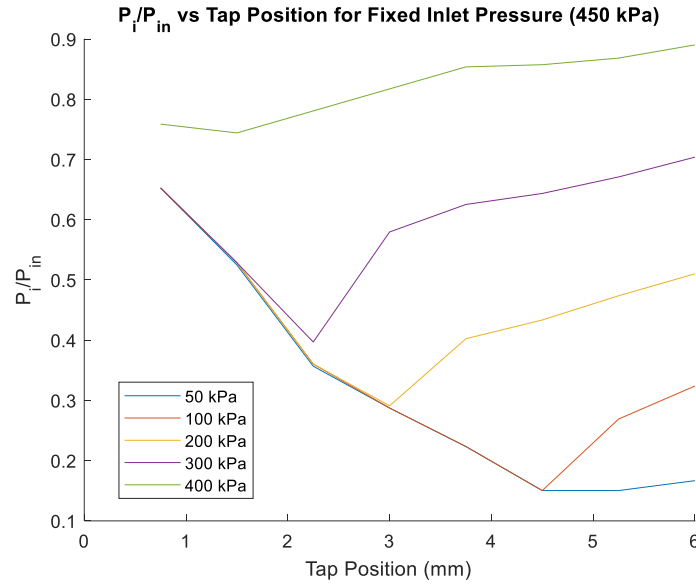


**Fig. 3 Pressure Ratio vs Tap Position for a Fixed Inlet Pressure of 450 Kpa.**

In Figure 3 where inlet pressure was held constant at 450 kPa, the back pressure is relatively close to the inlet pressure for the case where back pressure was 400 kPa. Because the ratio between inlet and outlet pressure is not large enough the flow is not choked so it does not form a shock and just exhibits properties of subsonic flow. However, for the 100, 200, or 300 kPa cases a shock forms, this is apparent as the ratio switches from decreasing and begins to increase after the shock abruptly. A shock forms when the flow has reached Mach at the throat of the test section also known as choked flow. As the pressure ratio gets smaller ( $P_{out} < P_{in}$ ) meaning there is a larger pressure difference between the inlet and outlet there are obvious signs of a shock forming. A large spike upwards in the graph is evidence of a shock being formed. The only case for a fixed outlet pressure in which a shock doesn't form is when the outlet pressure is 50 kPa. The ratio just continues to decrease along the taps, meaning no shock has formed and so the flow is just supersonic all the way through with no shock to slow it down to subsonic and thus increase the outlet pressure. It is also worth highlighting that a trend appears as the initial pressure ratio increases the shock forms farther down the nozzle meaning there is a correlation between pressure ratio and location of shock formation within the nozzle.

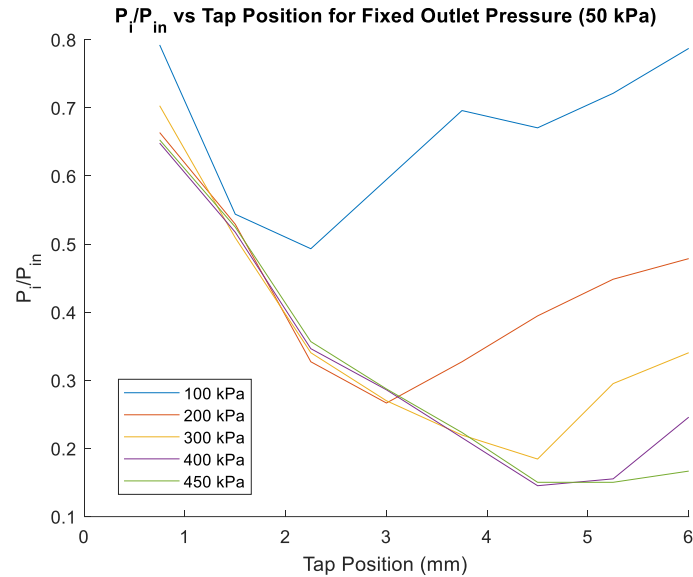


**Fig. 4 Pressure Ratio vs Tap Position for a Fixed outlet Pressure of 50 Kpa.**

In Figure 4, where outlet pressure was held constant at 50 kPa the same observations as Fig. 3 are apparent. Holding the outlet at 50 kPa and an inlet pressure of 450 kPa produces an identical curve to the last case from Fig. 3. The flow is choked and supersonic but choked flow does not guarantee a shock will form in the nozzle, so there is no shock present. The three cases in between are all similar solidifying the trend that as the pressure ratio increases between inlet and outlet ( $P_{in} > P_{out}$ ) so does the distance the shock forms. For the case in which inlet is 100 kPa the flow is once again not reaching the choked flow and stays subsonic, so a shock is not present. This is more obvious when looking at Table 1 as the velocity at station 1 and 8 are basically the same.

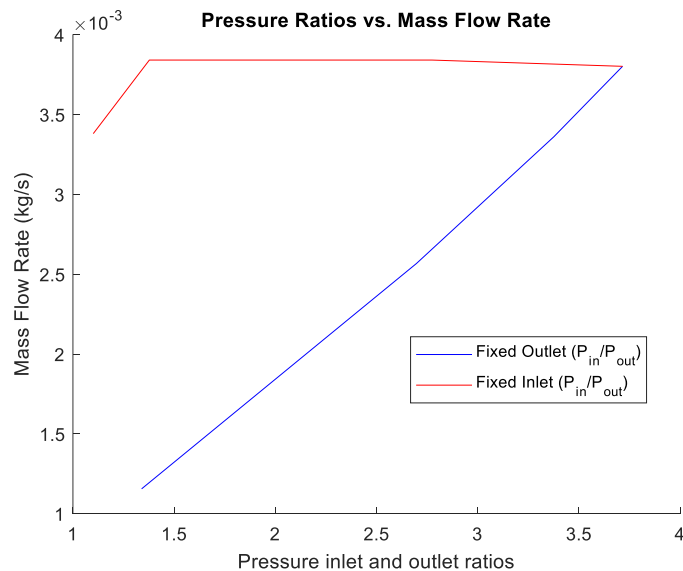


**Fig. 5 Pressure Ratio vs. Mass Flow Rate.**

In Figure 5, mass flow rate stays constant with the fixed inlet pressure whereas with a fixed outlet pressure the mass flow rate increases in what seems to be a linear fashion. The reason there is a little area at the beginning of the fixed inlet that is not constant is because the flow at this pressure ratio is not choked yet and up until choked flow the outlet pressure does affect the mass flow rate. Whereas it's obvious once the flow is choked the mass flow rate is only affected by varying the inlet pressure this is why for the fixed inlet the flow remains constant once choked, this

aligns with choked flow assumptions. The choked flow area for this nozzle seems to be around  $1.3 P_{in}/P_{out}$  for this geometry.

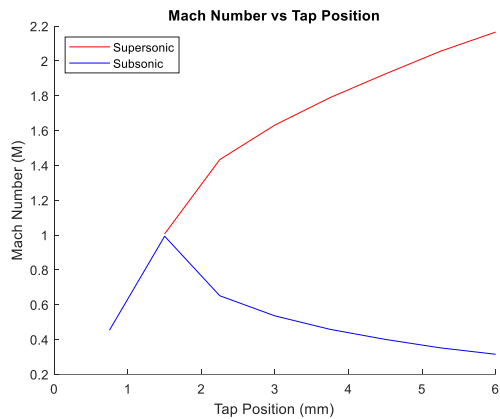


**Fig. 7 Mach Number vs Tap Position.**

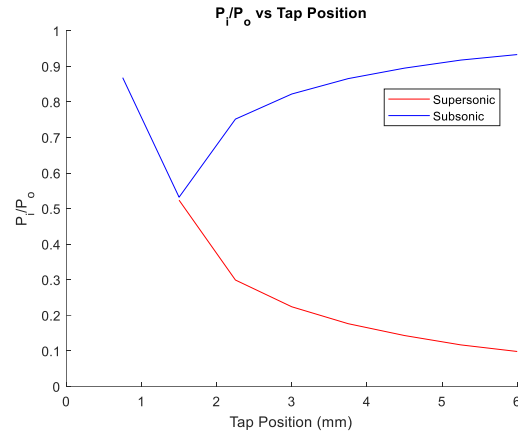


**Fig. 7 Pressure Ratio vs Tap Position.**

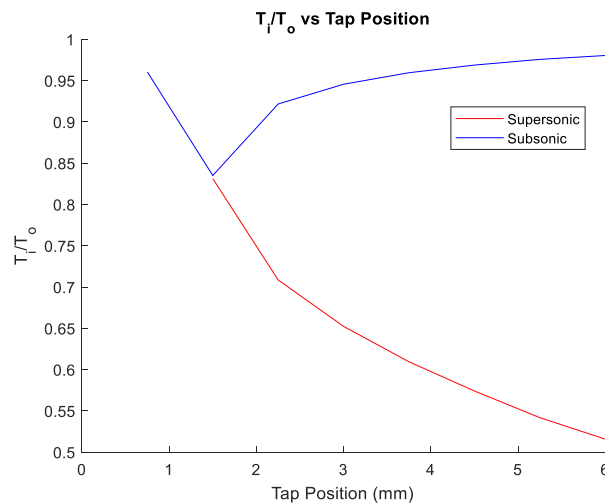


**Fig. 8 Temperature Ratio vs Tap Position.**

Figures (6-8) all depict the theoretical cases the flow can have in a nozzle, for both cases up until the throat of the nozzle the mass flow rate acts the same as both cases are subsonic. However, if the flow can reach Mach ( $M = 1$ ) in the throat, then the flow is supersonic, and the mass flow rate increases as the velocity speeds up within the nozzle past the throat. Supersonic flow has an increase in velocity and is compressible as the nozzle diverges and area increases. If the flow doesn't reach  $M = 1$  at the throat, then mass flow rate decreases back to about what it was at the inlet because the nozzle is expanding, and the flow is subsonic meaning it decreases with a larger area. For Figures (7-8), the pressure and temperature theoretical plots, it is apparent that as Mach increases pressure and temperature decreases and vice versa. It is also important to highlight although these are theoretical plots, the critical pressure ratio of about 1.3 is the point at which the flow will become choked if the flow reaches  $M = 1$ .

**Table 1. Experimental Data**

	Variable Pressure (Kpa)	Speed of Sound (m/s)		Density (kg/m <sup>3</sup> )		Velocity (m/s)	
		Station 1	Station 8	Station 1	Station 8	Station 1	Station 8
Fixed outlet Pressure (kPa)  50 kPa	100	343.78	344.662	1.845	1.833	138.488	139.380
	200	344.08	344.370	2.329	1.680	254.378	352.697
	300	344.08	344.312	3.298	1.597	218.466	450.980
	400	344.08	344.079	3.806	1.444	220.156	580.182
	450	344.08	344.079	4.219	1.078	200.871	786.101
Fixed Inlet Pressure (kPa)  450 kPa	50	344.079	344.0790	4.2194	1.0781	199.2002	779.564
	100	344.079	344.079	4.219	2.093	289.805	584.024
	200	344.079	344.079	4.219	3.298	255.509	326.865
	300	344.079	344.079	4.219	4.550	226.960	210.466
	400	344.079	344.079	4.904	5.754	153.665	130.960

**Table 2. Force on Nozzle**

	Ratio of Inlet Pressure over Outlet Pressure	Force of Fluid on Nozzle (N)
Fixed Outlet Pressure (50 kPa)	2	-0.1846
	4	0.6185
	6	1.7109
	8	2.8479
	9	4.3613
Fixed Inlet Pressure (450 kPa)	9	4.3066
	4.5	3.2953
	2.25	0.8170
	1.5	-0.4902
	1.125	-1.0209

Observing Table 2; the force on the nozzle increases as the pressure ratio increases, meaning there is a correlation between the two. Force reaches its maximum as the ratio of pressure difference reaches the highest tested value too. It seems a shockwave is also affecting the force based on fixed inlet pressure scenario where the pressure ratio of 4.5

has a higher force than the pressure ratio of 8 for fixed outlet pressure. This phenomenon indicates that the presence of a shock wave must be increasing the force on the nozzle. However, with this limited test case and data it is not certain if the shockwave is the only contributing factor, there are other factors such as density, velocity, and pressure at the entrance and exit that will also play a role in force generated. It is also not apparent if the location of the shock has an effect as there are not enough points to analyze for this case to know for sure.

**Table 3. Bernoulli's Equation**

	Ratio of Inlet Pressure over Outlet Pressure	Pressure Difference Between Left and Right side (%)
Fixed Outlet Pressure (50 kPa)	2	0.5105
	4	9.9569
	6	18.3680
	8	12.6063
	9	4.1505
Fixed Inlet Pressure (450 kPa)	9	5.1393
	4.5	0.0209
	2.25	8.3185
	1.5	4.2230
	1.125	12.5651

Table 3 represents calculations using Bernoulli's Equation and as expected Bernoulli's equation does not hold up in compressible flow conditions. If the flow was incompressible there would be an obvious correlation between an increase in pressure ratio and an increase in pressure difference between the left-hand and right-hand side of the valve. The reason Bernoulli's doesn't hold up is the assumption within its derivation that the flow is incompressible, meaning any result past Mach is going to be highly inaccurate. In Table 3 the pressure difference grows erratically jumping up and down, this confirms that Bernoulli's Is not an accurate analysis method for this experiment.

**Table 4. Shock Formation in Nozzle**

	Ratio of Inlet Pressure over Outlet Pressure	Theoretical Shock Location (in terms of area mm <sup>2</sup> )	Actual Shock Location from Experimental Data (mm <sup>2</sup> )
Fixed Outlet Pressure (50 kPa)	2	N/A since $M_s < 1$	N/A since $M_s < 1$
	4	5.97141	4.012 < Area < 4.486
	6	8.50159	4.988 < Area < 5.557
	8	13.14159	5.557 < Area < 6.113
	9	N/A	N/A
Fixed Inlet Pressure (450 kPa)	9	N/A	N/A
	4.5	3.14159	4.988 < Area < 5.557
	2.25	3.43031	4.012 < Area < 4.486
	1.5	3.33552	3.563 < Area < 4.012
	1.125	N/A since $M_s < 1$	N/A since $M_s < 1$

The theoretical shock locations shown in Table 4 are very likely to be inaccurate due to some data analysis errors here as the shock would be unable to form before the throat. It should also be noted that errors are likely present in the calculations due to some of the theoretical shock areas being larger than the C-D nozzle areas. However, in the sections where the flow reached Mach 1, it is apparent where the shocks have formed as there are very large pressure jumps between the pressure taps where the shock has most likely formed. There is a correlation between where the shock seems to form and the pressure ratio decreasing for the fixed inlet pressure scenario. As the pressure ratio decreases, the area of the section where the shock has formed decreases, meaning the location of the shock is moving nearer to the throat with a decrease in pressure ratio. This is why in some cases where the pressure ratio is very high or very low there is not a shock present within the nozzle as for the fixed outlet case with a ratio of 2 the flow never reaches Mach. Whereas when the ratio is 9 for both the fixed outlet and inlet case the flow is supersonic all the way through the nozzle as no shock forms within the nozzle. The last case for the fixed inlet is when the pressure ratio is very small – roughly 1.125 – and the flow does not reach the choked condition, so it is subsonic and no shock forms.

## V. Conclusions

This experiment successfully showed the measurable behaviors of compressible flow in a nozzle. The data collected by this lab group confirmed that choked flow occurs when the flow speed reaches the speed of sound at the nozzle's throat but remains unchoked before achieving that speed. As the inlet-to-outlet pressure ratio increased, normal shocks appeared in the diverging section of the nozzle. When the outlet pressure was held constant, the shock's position was closely tied to the pressure ratio between the outlet and inlet on either side of the nozzle. At intermediate ratios, a shock was noticeable, but at very low or high ratios, the flow remained either fully subsonic or fully supersonic. The expected trend for the  $P_i/p_{in}$  plot was that it would show a sharp change in shock location as the flow transitions from subsonic to supersonic. In the experiment the shock position was observed to shift downstream with increasing pressure ratios across most of the test range and remained stationary at very low and high ratios, confirming the theoretical expectations with only minor deviations that can be attributed to experimental limitations such as sensor resolution and calibration.

Similarly, when the inlet pressure was held constant and the outlet pressure adjusted, the shock shifted, with lower outlet pressures pulling it closer to the throat, consistent with theoretical predictions. The relationship between shock position and pressure ratio was clearly observed, with the shock moving downstream at higher pressure ratios and closer to the throat at lower ones. Once the flow velocity reached the critical point at Mach 1 and became choked, the mass flow rate remained constant, even when the outlet pressure was further reduced, aligning well with theoretical expectations. The mass flow rate through the nozzle was expected to remain constant after choking, and this was confirmed in the experiment. A more detailed examination of how the mass flow rate varies with pressure ratio before choking, including a quantitative description of these changes, would have provided further insight into the flow dynamics before critical conditions are reached, however, that was outside the scope of this lab experiment but could be implemented in the future to provide a deeper understanding.

Force measurements on the nozzle showed the shock significantly altered the structural load within the nozzle. These shocks created substantial forces that, if applied to a larger test radius or weaker material, could have led to structural damage or failure. The force measurements indicated a substantial variation in the nozzle's structural load, especially in the diverging section where the shock waves were present. The magnitude of these forces is critical in the design of a nozzle in practical use where material failure is a risk. The experimental data showed that shocks could generate peak forces of 4.36 N, which while small in this experiment could severely impact nozzle integrity if not properly accounted for in the design of a larger and less stiff system.

Attempting to measure any of the forces or other system variables using Bernoulli's equation yielded predictions that were significantly off from the experimental measurements. This discrepancy is because Bernoulli's equation does not account for changes in fluid density, which is most significant in compressible flow. As the velocity of the flow approached supersonic speeds, density variations had a considerable impact on the results, making Bernoulli's equation ineffective for predicting the experimental outcomes accurately. The flow speed was too high to be meaningfully analyzed by Bernoulli's equation.

This lab supported the core principles of isentropic flow and shock dynamics, providing valuable insights into how pressure, density, velocity, and temperature interact in high-speed/compressible flows. The experimental results largely confirmed the theoretical models for shock behavior, but some discrepancies in shock position suggest that data collection and analysis were affected by tool calibration and instrument specificity. These minor deviations between the theoretical predictions and experimental results can likely be attributed to sensor resolution and the calibration of the measurement devices. To improve the accuracy of future experiments, it would be beneficial to use

higher-resolution pressure transducers, especially in detecting smaller pressure gradients near the shock, and to explore a broader range of experimental conditions to gain more comprehensive data on compressible flow behavior. Expanding the range of nozzle area ratios or testing with different gases could provide a more thorough understanding of how nozzle design influences shock formation and flow characteristics. Incorporating these improvements would enable a more accurate analysis of compressible nozzle flow, which is crucial for the aerospace industry. This understanding could lead to advancements in engines, rocket nozzles, and the overall efficiency of supersonic aircraft.

## Appendix A: Tabular Results

**Table A1 – Density & Uncertainty**

Varying Pressure	Position	Density (Kg/m <sup>3</sup> )	Density Uncertainty (Kg/m <sup>3</sup> )
Varying Inlet Fixed Outlet			
100	1	1.8458	0.0064
100	2	1.2671	0.0045
100	3	1.149	0.0041
100	4	1.3852	0.0048
100	5	1.6214	0.0056
100	6	1.5624	0.0054
100	7	1.6805	0.0058
100	8	1.834	0.0063
200	1	2.33	0.008
200	2	1.8576	0.0064
200	3	1.149	0.0041
200	4	0.9365	0.0034
200	5	1.149	0.0041
200	6	1.3852	0.0048
200	7	1.5742	0.0055
200	8	1.6805	0.0058
300	1	3.2983	0.0112
300	2	2.389	0.0082
300	3	1.5978	0.0055
300	4	1.2671	0.0045
300	5	1.0309	0.0037
300	6	0.8656	0.0032
300	7	1.3852	0.0048
300	8	1.5978	0.0055
400	1	3.8061	0.0129
400	2	3.0385	0.0104
400	3	2.0347	0.007
400	4	1.6805	0.0058
400	5	1.2671	0.0045
400	6	0.8538	0.0031
400	7	0.9129	0.0033
400	8	1.4443	0.005
450	1	4.2194	0.0143
450	2	3.3928	0.0116
450	3	2.3063	0.0079
450	4	1.8576	0.0064
450	5	1.4443	0.005
450	6	0.9719	0.0035
450	7	0.9719	0.0035
450	8	1.0782	0.0038
Varying Outlet Fixed Inlet			



50	1	4.2194	0.0143
50	2	3.4164	0.0116
50	3	2.33	0.008
50	4	1.8576	0.0064
50	5	1.4443	0.005
50	6	0.9719	0.0035
50	7	1.7395	0.006
50	8	2.0938	0.0072
100	1	4.2194	0.0143
100	2	3.4164	0.0116
100	3	2.33	0.008
100	4	1.8812	0.0065
100	5	2.6016	0.0089
100	6	2.8023	0.0096
100	7	3.0621	0.0104
100	8	3.2983	0.0112
200	1	4.2194	0.0143
200	2	3.4164	0.0116
200	3	2.5662	0.0088
200	4	3.7471	0.0127
200	5	4.0423	0.0137
200	6	4.1604	0.0141
200	7	4.3375	0.0147
200	8	4.5501	0.0155
300	1	4.9044	0.0167
300	2	4.8099	0.0163
300	3	5.0461	0.0171
300	4	5.2823	0.0179
300	5	5.5185	0.0187
300	6	5.5421	0.0188
300	7	5.6129	0.019
300	8	5.7546	0.0195

**Table A2** – Original Data

Fixed Pressure	Variable Pressure [kPa]	$p_1$ [kPa]	$p_2$ [kPa]	$p_3$ [kPa]	$p_4$ [kPa]	$p_5$ [kPa]	$p_6$ [kPa]	$p_7$ [kPa]	$p_8$ [kPa]	$T_{in}$ [°C]	$T_{out}$ [°C]	$\dot{m}$ [g/s]	$p_{atm}$ [kPa]	$T_{atm}$ [°C]
Outlet 50kPa	100	59	10	0	20	40	35	45	58	21	22.5	1.18	97.3	21.9
	200	100	60	0	-18	0	20	36	45	21.5	22	1.9		
	300	182	105	38	10	-10	-24	20	38	21.5	21.9	2.62		
	400	225	160	75	45	10	-25	-20	25	21.5	21.5	3.43		
	450	260	190	98	60	25	-15	-15	-6	21.5	21.5	3.88		
Inlet 450kPa	50	260	190	98	60	25	-15	-15	-6	21.5	21.5	3.88	97.3	21.9
	100	260	192	100	60	25	-15	50	80	21.5	21.5	3.92		
	200	260	192	100	62	123	140	162	182	21.5	21.5	3.92		
	300	260	192	120	220	245	255	270	288	21.5	21.5	3.92		

	400	318	310	330	350	370	372	378	390	22	21.5	3.45		
--	-----	-----	-----	-----	-----	-----	-----	-----	-----	----	------	------	--	--

**Table A3 – Theoretical Plots Data**

Tap Position (mm)	0.75	1.5	2.25	3	3.75	4.5	5.25	6
Mach Supersonic	0.4535	1.007	1.4338	1.6322	1.7898	1.9256	2.0559	2.1662
Mach Subsonic	0.4535	0.9934	0.6515	0.5359	0.4586	0.4008	0.3521	0.3155
Pressure Ratio Supersonic	0.8684	0.524	0.2996	0.2243	0.1768	0.1434	0.1171	0.0986
Pressure Ratio Subsonic	0.8684	0.5323	0.7519	0.8225	0.8657	0.8952	0.9178	0.9333
Temperature Ratio Supersonic	0.9605	0.8314	0.7086	0.6524	0.6095	0.5742	0.5419	0.5159
Temperature Ratio Subsonic	0.9605	0.8352	0.9218	0.9457	0.9596	0.9689	0.9758	0.9805

## Appendix B: Sample Calculations

### B.1 Calculation of Density

$$\rho = \frac{p}{RT} \quad (2)$$

$$\rho = \frac{97.085}{296.35 \cdot 0.287} = 1.1415 \text{ kg/m}^3$$

### B.2 Calculation of Density Uncertainty

$$\delta\rho = \sqrt{\left(\frac{1}{RT} \cdot \delta p\right)^2 + \left(\frac{p}{RT^2} \cdot \delta T\right)^2} \quad (3)$$

$$\delta\rho = \sqrt{\left(\frac{0.1}{0.287 \cdot 296.35}\right)^2 + \left(\frac{96.085 \cdot 1}{0.287 \cdot 296.35^2}\right)^2} = 0.0040 \text{ kg/m}^3$$

### B.3 Calculation of Speed of Sound

$$a = \sqrt{\gamma RT} \quad (8)$$

$$a = \sqrt{1.4 \cdot 287 \cdot 296.35} = 345.07 \text{ m/s}$$

### B.4 Calculation of Mach Number

$$M = \frac{u}{a} \quad (9)$$

$$M = \frac{580.182}{345.07} = 1.681$$

#### B.5 Calculation of Isentropic Temperature Ratio

$$\frac{T_0}{T} = \left[ 1 + \frac{\gamma - 1}{2} M^2 \right] \quad (10.1)$$

$$\frac{T_0}{T} = 1 + \frac{(1.4 - 1)}{2} (1.681)^2 = 1.565$$

#### B.6 Calculation of Isentropic Pressure Ratio

$$\frac{p_0}{p} = \left[ 1 + \frac{\gamma - 1}{2} M^2 \right]^{\frac{\gamma}{\gamma - 1}} \quad (10.2)$$

$$\frac{p_0}{p} = \left[ 1 + \frac{(1.4 - 1)}{2} (1.681)^2 \right]^{\frac{1.4}{1.4 - 1}} = 4.797$$

#### B.7 Calculation of Isentropic Density Ratio

$$\frac{\rho_0}{\rho} = \left[ 1 + \frac{\gamma - 1}{2} M^2 \right]^{\frac{1}{\gamma - 1}} \quad (10.3)$$

$$\frac{\rho_0}{\rho} = \left[ 1 + \frac{(1.4 - 1)}{2} (1.681)^2 \right]^{\frac{1}{1.4 - 1}} = 3.065$$

#### B.8 Calculation of Pressure Ratio Across a Shock

$$\frac{p_2}{p_1} = 1 + \frac{2\gamma}{\gamma + 1} (M_1^2 - 1) \quad (13.1)$$

$$\frac{p_2}{p_1} = 1 + \frac{2 \cdot 1.4}{1.4 + 1} \cdot ((1.681)^2 - 1) = 3.130$$

#### B.9 Calculation of Density Ratio Across a Shock

$$\frac{\rho_2}{\rho_1} = \frac{(\gamma + 1)M_1^2}{2 + (\gamma - 1)M_1^2} \quad (13.2)$$

$$\frac{\rho_2}{\rho_1} = \frac{(1.4 + 1) \cdot (1.681)^2}{2 + (1.4 - 1) \cdot (1.681)^2} = 2.167$$

#### B.10 Calculation of Mach Across a Shock

$$M_2^2 = \frac{1 + \frac{\gamma - 1}{2} M_1^2}{\gamma M_1^2 - \frac{\gamma - 1}{2}} \quad (13.3)$$

$$M_2^2 = \frac{1 + \frac{(1.4 - 1)}{2} \cdot (1.681)^2}{(1.4 \cdot (1.681)^2 - \frac{(1.4 - 1)}{2})} = 0.417$$

#### B.11 Calculation of Temperature Ratio Across a Shock

$$\frac{T_2}{T_1} = \frac{p_2}{p_1} \cdot \frac{\rho_1}{\rho_2} \quad (13.4)$$

$$\frac{T_2}{T_1} = 3.13 \cdot 2.167 = 6.781$$

### Appendix C: MATLAB Code

%% Importing Data and Defining Elements

T = 22 + 273.15;

```
files = xlsread("C:\Users\traen\Downloads\AEE362 Lab 2 Data.xlsx");
files = files(:, 1:end-2); % Remove the last two columns
tapposition = [0.75 1.5 2.25 3 3.75 4.5 5.25 6]; % Position of taps 1-8 (mm)
tapdiameters = [2.4 2 2.13 2.26 2.39 2.52 2.66 2.79] .* 0.001; % Diameter of taps 1-8 (m)
tapareas = (pi/4).*tapdiameters.^2; % Areas for taps 1-8 (m^2)
patm = 97.3; % kPa
outletfixedP = 50 + patm; % kPa
inletfixedP = 450 + patm; % kPa
Tatm = 21.9 + 273.15; % K
gamma = 1.4;
R = 287; % J/kg*K
Athroat = tapareas(2); % Area of throat in m^2 (throat diameter is taken from lab manual)
varyingInletData = files(1:5, :); % Separating varying inlet data
varyingOutletData = files(6:10, :); % Separating varying outlet data
```

%% Varying Inlet Pressure Calculations

%P1-P8 for each varying inlet pressure (kPa)

```
Pinletvar = varyingInletData(:,1) + patm;
pi100varin = varyingInletData(1,2:9) + patm;
pi200varin = varyingInletData(2, 2:9) + patm;
pi300varin = varyingInletData(3, 2:9) + patm;
pi400varin = varyingInletData(4, 2:9) + patm;
pi450varin = varyingInletData(5, 2:9) + patm;
```

%Density for stations 1-8 using varying inlet pressure (kg/m^3)

```
rho100inletvar = pi100varin.*(1000)./(R.*Tatm);
rho200inletvar = pi200varin.*(1000)./(R.*Tatm);
rho300inletvar = pi300varin.*(1000)./(R.*Tatm);
rho400inletvar = pi400varin.*(1000)./(R.*Tatm);
rho450inletvar = pi450varin.*(1000)./(R.*Tatm);
```

%Temperature for varying inlet pressure data (K)

```
Tempinletvarin = varyingInletData(:,10) + 273.15;
Tempoutletvarin = varyingInletData(:,11) + 273.15;
```

%Mass flow rate for varying inlet pressure(kg/s)

```
mdotvarin = varyingInletData(:,12).*0.98.*0.001;
```

%Speed of sound for varying inlet pressure (m/s)

```
a = sqrt(gamma*R*T);
```

%Velocity of stations 1-8 for varying inlet pressure (m/s)

```
velocity100varin = mdotvarin(1)./(rho100inletvar.*tapareas(1));
velocity200varin = mdotvarin(2)./(rho200inletvar.*tapareas(2));
velocity300varin = mdotvarin(3)./(rho300inletvar.*tapareas(3));
velocity400varin = mdotvarin(4)./(rho400inletvar.*tapareas(4));
velocity450varin = mdotvarin(5)./(rho450inletvar.*tapareas(5));
```

%Mach numbers of stations 1-8 for varying inlet pressure

```
M100varin = velocity100varin./a;
M200varin = velocity200varin./a;
M300varin = velocity300varin./a;
```

M400varin = velocity400varin./a;  
M450varin = velocity450varin./a;

%Force of Fluid on Nozzle for varying inlet pressure (fixed outlet pressure) (N)

Fext100varin = -rho100inletvar(1)\*velocity100varin(1)^2\*tapareas(1) + ...  
rho100inletvar(8)\*velocity100varin(8)^2\*tapareas(8) + pi100varin(1)\*1000\*tapareas(1) -  
pi100varin(8)\*1000\*tapareas(8);  
Fext200varin = -rho200inletvar(1)\*velocity200varin(1)^2\*tapareas(1) + ...  
rho200inletvar(8)\*velocity200varin(8)^2\*tapareas(8) + pi200varin(1)\*1000\*tapareas(1) -  
pi200varin(8)\*1000\*tapareas(8);  
Fext300varin = -rho300inletvar(1)\*velocity300varin(1)^2\*tapareas(1) + ...  
rho300inletvar(8)\*velocity300varin(8)^2\*tapareas(8) + pi300varin(1)\*1000\*tapareas(1) -  
pi300varin(8)\*1000\*tapareas(8);  
Fext400varin = -rho400inletvar(1)\*velocity400varin(1)^2\*tapareas(1) + ...  
rho400inletvar(8)\*velocity400varin(8)^2\*tapareas(8) + pi400varin(1)\*1000\*tapareas(1) -  
pi400varin(8)\*1000\*tapareas(8);  
Fext450varin = -rho450inletvar(1)\*velocity450varin(1)^2\*tapareas(1) + ...  
rho450inletvar(8)\*velocity450varin(8)^2\*tapareas(8) + pi450varin(1)\*1000\*tapareas(1) -  
pi450varin(8)\*1000\*tapareas(8);

%Percent Difference between LHS and RHS for varying Inlet/constant outlet

LHS100varin = pi100varin(1).\*1000 + 0.5\*rho100inletvar(1)\*velocity100varin(1)^2;  
RHS100varin = pi100varin(8).\*1000 + 0.5\*rho100inletvar(8)\*velocity100varin(8)^2;

LHS200varin = pi200varin(1).\*1000 + 0.5\*rho200inletvar(1)\*velocity200varin(1)^2;  
RHS200varin = pi200varin(8).\*1000 + 0.5\*rho200inletvar(8)\*velocity200varin(8)^2;

LHS300varin = pi300varin(1).\*1000 + 0.5\*rho300inletvar(1)\*velocity300varin(1)^2;  
RHS300varin = pi300varin(8).\*1000 + 0.5\*rho300inletvar(8)\*velocity300varin(8)^2;

LHS400varin = pi400varin(1).\*1000 + 0.5\*rho400inletvar(1)\*velocity400varin(1)^2;  
RHS400varin = pi400varin(8).\*1000 + 0.5\*rho400inletvar(8)\*velocity400varin(8)^2;

LHS450varin = pi450varin(1).\*1000 + 0.5\*rho450inletvar(1)\*velocity450varin(1)^2;  
RHS450varin = pi450varin(8).\*1000 + 0.5\*rho450inletvar(8)\*velocity450varin(8)^2;

percentdiff100varin = abs(LHS100varin - RHS100varin) / ((abs(LHS100varin) + abs(RHS100varin)) / 2) \* 100;  
percentdiff200varin = abs(LHS200varin - RHS200varin) / ((abs(LHS200varin) + abs(RHS200varin)) / 2) \* 100;  
percentdiff300varin = abs(LHS300varin - RHS300varin) / ((abs(LHS300varin) + abs(RHS300varin)) / 2) \* 100;  
percentdiff400varin = abs(LHS400varin - RHS400varin) / ((abs(LHS400varin) + abs(RHS400varin)) / 2) \* 100;  
percentdiff450varin = abs(LHS450varin - RHS450varin) / ((abs(LHS450varin) + abs(RHS450varin)) / 2) \* 100;

%Finding P08 and P01 for Varying inlet/constant outlet pressure

Po100varin1 = pi100varin(1)\*(1 + ((gamma - 1)/2)\*M100varin(1)^2)^(gamma/(gamma-1));  
Po100varin8 = pi100varin(8)\*(1 + ((gamma - 1)/2)\*M100varin(8)^2)^(gamma/(gamma-1));

Po200varin1 = pi200varin(1)\*(1 + ((gamma - 1)/2)\*M200varin(1)^2)^(gamma/(gamma-1));  
Po200varin8 = pi200varin(8)\*(1 + ((gamma - 1)/2)\*M200varin(8)^2)^(gamma/(gamma-1));

Po300varin1 = pi300varin(1)\*(1 + ((gamma - 1)/2)\*M300varin(1)^2)^(gamma/(gamma-1));  
Po300varin8 = pi300varin(8)\*(1 + ((gamma - 1)/2)\*M300varin(8)^2)^(gamma/(gamma-1));

Po400varin1 = pi400varin(1)\*(1 + ((gamma - 1)/2)\*M400varin(1)^2)^(gamma/(gamma-1));  
Po400varin8 = pi400varin(8)\*(1 + ((gamma - 1)/2)\*M400varin(8)^2)^(gamma/(gamma-1));

Po450varin1 = pi450varin(1)\*(1 + ((gamma - 1)/2)\*M450varin(1)^2)^(gamma/(gamma-1));

Po450varin8 = pi450varin(8)\*(1 + ((gamma - 1)/2)\*M450varin(8)^2)^(gamma/(gamma-1));

PinPoutratiofixedout = Pinletvar./outletfixedP; %% ASK IF USE GAGE PRESSURE OR ACTUAL PRESSURE!!

%% Varying Outlet Pressure Calculations

%P1-P8 for each varying outlet pressure (kPa)

Poutletvar = varyingOutletData(:,1) + patm;

pi50varout = varyingOutletData(1,2:9) + patm;

pi100varout = varyingOutletData(2, 2:9) + patm;

pi200varout = varyingOutletData(3, 2:9) + patm;

pi300varout = varyingOutletData(4, 2:9) + patm;

pi400varout = varyingOutletData(5, 2:9) + patm;

%Density for stations 1-8 using varying inlet pressure (kg/m^3)

rho50outletvar = pi50varout.\*(1000)./(R.\*Tatm);

rho100outletvar = pi100varout.\*(1000)./(R.\*Tatm);

rho200outletvar = pi200varout.\*(1000)./(R.\*Tatm);

rho300outletvar = pi300varout.\*(1000)./(R.\*Tatm);

rho400outletvar = pi400varout.\*(1000)./(R.\*Tatm);

%Temperature for varying outlet pressure data (K)

Tempinletvarout = varyingOutletData(:,10) + 273.15;

Tempoutletvarout = varyingOutletData(:,11) + 273.15;

%Mass flow rate for varying outlet pressure (kg/s)

mdotvarout = varyingOutletData(:,12).\*0.98.\*0.001;

%Velocity of stations 1-8 for varying inlet pressure (m/s)

velocity50varout = mdotvarout(1)./(rho50outletvar.\*tapareas(1));

velocity100varout = mdotvarout(2)./(rho100outletvar.\*tapareas(2));

velocity200varout = mdotvarout(3)./(rho200outletvar.\*tapareas(3));

velocity300varout = mdotvarout(4)./(rho300outletvar.\*tapareas(4));

velocity400varout = mdotvarout(5)./(rho400outletvar.\*tapareas(5));

%Mach numbers of stations 1-8 for varying outlet pressure

M50varout = velocity50varout./a;

M100varout = velocity100varout./a;

M200varout = velocity200varout./a;

M300varout = velocity300varout./a;

M400varout = velocity400varout./a;

%Force of Fluid on Nozzle for varying inlet pressure (fixed outlet pressure) (N)

Fext50varout = -rho50outletvar(1)\*velocity50varout(1)^2\*tapareas(1) + ...

rho50outletvar(8)\*velocity50varout(8)^2\*tapareas(8) + pi50varout(1)\*1000\*tapareas(1) -  
pi50varout(8)\*1000\*tapareas(8);

Fext100varout = -rho100outletvar(1)\*velocity100varout(1)^2\*tapareas(1) + ...

rho100outletvar(8)\*velocity100varout(8)^2\*tapareas(8) + pi100varout(1)\*1000\*tapareas(1) -  
pi100varout(8)\*1000\*tapareas(8);

Fext200varout = -rho200outletvar(1)\*velocity200varout(1)^2\*tapareas(1) + ...

rho200outletvar(8)\*velocity200varout(8)^2\*tapareas(8) + pi200varout(1)\*1000\*tapareas(1) -  
pi200varout(8)\*1000\*tapareas(8);

Fext300varout = -rho300outletvar(1)\*velocity300varout(1)^2\*tapareas(1) + ...

rho300outletvar(8)\*velocity300varout(8)^2\*tapareas(8) + pi300varout(1)\*1000\*tapareas(1) -  
pi300varout(8)\*1000\*tapareas(8);

Fext400varout = -rho400outletvar(1)\*velocity400varout(1)^2\*tapareas(1) + ...

```
rho400outletvar(8)*velocity400varout(8)^2*tapareas(8) + pi400varout(1)*1000*tapareas(1) -
pi400varout(8)*1000*tapareas(8);
```

```
%Percent Difference between LHS and RHS for varying Inlet/constant outlet
```

```
LHS50varout = pi50varout(1).*1000 + 0.5*rho50outletvar(1)*velocity50varout(1)^2;
```

```
RHS50varout = pi50varout(8).*1000 + 0.5*rho50outletvar(8)*velocity50varout(8)^2;
```

```
LHS100varout = pi100varout(1).*1000 + 0.5*rho100outletvar(1)*velocity100varout(1)^2;
```

```
RHS100varout = pi100varout(8).*1000 + 0.5*rho100outletvar(8)*velocity100varout(8)^2;
```

```
LHS200varout = pi200varout(1).*1000 + 0.5*rho200outletvar(1)*velocity200varout(1)^2;
```

```
RHS200varout = pi200varout(8).*1000 + 0.5*rho200outletvar(8)*velocity200varout(8)^2;
```

```
LHS300varout = pi300varout(1).*1000 + 0.5*rho300outletvar(1)*velocity300varout(1)^2;
```

```
RHS300varout = pi300varout(8).*1000 + 0.5*rho300outletvar(8)*velocity300varout(8)^2;
```

```
LHS400varout = pi400varout(1).*1000 + 0.5*rho400outletvar(1)*velocity400varout(1)^2;
```

```
RHS400varout = pi400varout(8).*1000 + 0.5*rho400outletvar(8)*velocity400varout(8)^2;
```

```
percentdiff50varout = abs(LHS50varout - RHS50varout) / ((abs(LHS50varout) + abs(RHS50varout)) / 2) * 100;
```

```
percentdiff100varout = abs(LHS100varout - RHS100varout) / ((abs(LHS100varout) + abs(RHS100varout)) / 2) *
100;
```

```
percentdiff200varout = abs(LHS200varout - RHS200varout) / ((abs(LHS200varout) + abs(RHS200varout)) / 2) *
100;
```

```
percentdiff300varout = abs(LHS300varout - RHS300varout) / ((abs(LHS300varout) + abs(RHS300varout)) / 2) *
100;
```

```
percentdiff400varout = abs(LHS400varout - RHS400varout) / ((abs(LHS400varout) + abs(RHS400varout)) / 2) *
100;
```

```
%Finding P08 and P01 for Varying outlet/constant inlet pressure
```

```
Po100varout1 = pi100varout(1)*(1 + ((gamma - 1)/2)*M100varout(1)^2)^(gamma/(gamma-1));
```

```
Po100varout8 = pi100varout(8)*(1 + ((gamma - 1)/2)*M100varout(8)^2)^(gamma/(gamma-1));
```

```
Po200varout1 = pi200varout(1)*(1 + ((gamma - 1)/2)*M200varout(1)^2)^(gamma/(gamma-1));
```

```
Po200varout8 = pi200varout(8)*(1 + ((gamma - 1)/2)*M200varout(8)^2)^(gamma/(gamma-1));
```

```
Po300varout1 = pi300varout(1)*(1 + ((gamma - 1)/2)*M300varout(1)^2)^(gamma/(gamma-1));
```

```
Po300varout8 = pi300varout(8)*(1 + ((gamma - 1)/2)*M300varout(8)^2)^(gamma/(gamma-1));
```

```
Po400varout1 = pi400varout(1)*(1 + ((gamma - 1)/2)*M400varout(1)^2)^(gamma/(gamma-1));
```

```
Po400varout8 = pi400varout(8)*(1 + ((gamma - 1)/2)*M400varout(8)^2)^(gamma/(gamma-1));
```

```
Po50varout1 = pi50varout(1)*(1 + ((gamma - 1)/2)*M50varout(1)^2)^(gamma/(gamma-1));
```

```
Po50varout8 = pi50varout(8)*(1 + ((gamma - 1)/2)*M50varout(8)^2)^(gamma/(gamma-1));
```

```
PinPoutratiofixedin = inletfixedP./Poutletvar; %% ASK IF USE GAGE OR ACTUAL PRESSURE!!
```

```
%% Graphs (CHECK FIRST ONE LATER)
```

```
%Mdot vs Pin/Pout Graph
```

```
figure;
```

```

hold on
plot(PinPoutratiofixedout,mdotvarin,'b')
plot(PinPoutratiofixedin,mdotvarout,'r')
xlabel('Pressure inlet and outlet ratios')
ylabel('Mass Flow Rate (kg/s)')
title('Pressure Ratios vs. Mass Flow Rate')
set(gcf,'color','white')
set(gca, 'Color', 'w')
legend('Fixed Outlet (P_i_n/P_o_u_t)','Fixed Inlet (P_o_u_t/P_i_n)','Location','best')

```

```

% Pi/Pin vs Tap Position Graph (Fixed inlet, varying outlet)
% ASK ABOUT IF IT LOOKS RIGHT!!
figure;
hold on
plot(tapposition, pi50varout/inletfixedP)
plot(tapposition, pi100varout/inletfixedP)
plot(tapposition, pi200varout/inletfixedP)
plot(tapposition, pi300varout/inletfixedP)
plot(tapposition, pi400varout/inletfixedP)
xlabel('Tap Position (mm)')
ylabel('P_i/P_i_n')
title('P_i/P_i_n vs Tap Position for Fixed Inlet Pressure (450 kPa)')
set(gcf,'color','white')
set(gca, 'Color', 'w')
legend('50 kPa','100 kPa','200 kPa','300 kPa','400 kPa','Location','best')
% Pi/Pin vs Tap Position Graph (Fixed outlet, varying inlet)
% ASK ABOUT IF IT LOOKS RIGHT AND IF IT IS Pi/Pout?
figure;
hold on
plot(tapposition, pi100varin ./ Pinletvar(1))
plot(tapposition, pi200varin ./ Pinletvar(2))
plot(tapposition, pi300varin ./ Pinletvar(3))
plot(tapposition, pi400varin ./ Pinletvar(4))
plot(tapposition, pi450varin ./ Pinletvar(5))
xlabel('Tap Position (mm)')
ylabel('P_i/P_i_n')
title('P_i/P_i_n vs Tap Position for Fixed Outlet Pressure (50 kPa)')
set(gcf,'color','white')
set(gca, 'Color', 'w')
legend('100 kPa','200 kPa','300 kPa','400 kPa','450 kPa','Location','best')

```

%% Table Values

```

%Speed of sound (fixed outlet pressure)
a1varin = sqrt(gamma.*R.*Tempinletvarin);
a8varin = sqrt(gamma.*R.*Tempoutletvarin);
%Speed of sound (fixed outlet pressure)
a1varout = sqrt(gamma.*R.*Tempoutletvarout);
a8varout = sqrt(gamma.*R.*Tempoutletvarout);

```

```

%Finding Ms from Po8 and Po1
p01inletvar = [Po100varin1 Po200varin1 Po300varin1 Po400varin1 Po450varin1];
p08inletvar = [Po100varin8 Po200varin8 Po300varin8 Po400varin8 Po450varin8];

```



```

% Initialize results array
Msvaluesinletvar = zeros(1, length(p01inletvar));

% Loop through each pair of p0 values
for i = 1:length(p01inletvar)
    % Define the equation as an anonymous function for each case
    Mseqinletvar = @(Ms) (((gamma+1).*Ms.^2)./((gamma-1).*Ms.^2 + 2)).^(gamma/(gamma-1)) * ...
        ((gamma+1)./(2*gamma.*Ms.^2 - (gamma-1))).^(1/(gamma-1)) - (p08inletvar(i)/p01inletvar(i));

    % Initial guess for fsolve
    guessinletvar = 1.5;

    % Solve for Mach number
    Msvaluesinletvar(i) = fsolve(Mseqinletvar, guessinletvar);
end

% Display results
disp('Solved Mach numbers:');
disp(Msvaluesinletvar);
%%
for i = 1:length(Msvaluesinletvar)
    Msinletvar = Msvaluesinletvar(i);
    Asvaluesinletvar(i) = Athroat * ((1 / Msinletvar) * ((2 / (gamma+1)) * (1 + ((gamma-1)/2) * Msinletvar^2)) ^
        ((gamma+1) / (2*(gamma-1))));
end
% Display results
disp('Computed shock areas (As):');
disp(Asvaluesinletvar);

%For Fixed inlet/varying outlet
p01outletvar = [Po50varout1 Po100varout1 Po200varout1 Po300varout1 Po400varout1];
p08outletvar = [Po50varout8 Po100varout8 Po200varout8 Po300varout8 Po400varout8];
%%
% Initialize results array
Msvaluesoutletvar = zeros(1, length(p01outletvar));

% Loop through each pair of p0 values
for i = 1:length(p01outletvar)
    % Define the equation as an anonymous function for each case
    Mseqoutletvar = @(Ms) (((gamma+1).*Ms.^2)./((gamma-1).*Ms.^2 + 2)).^(gamma/(gamma-1)) * ...
        ((gamma+1)./(2*gamma.*Ms.^2 - (gamma-1))).^(1/(gamma-1)) - (p08outletvar(i)/p01outletvar(i));

    % Initial guess for fsolve
    guessoutletvar = 1.5;

    % Solve for Mach number
    Msvaluesoutletvar(i) = fsolve(Mseqoutletvar, guessoutletvar);
end
Msvaluesoutletvar
% Display results
disp('Solved Mach numbers:');
disp(Msvaluesoutletvar);
%%
for i = 1:length(Msvaluesoutletvar)

```

```

    Msoutletvar = Msvaluesoutletvar(i);
    Asvaluesoutletvar(i) = Athroat * ((1 / Msoutletvar) * ((2 / (gamma+1)) * (1 + ((gamma-1)/2) * Msoutletvar^2)) ^
((gamma+1) / (2*(gamma-1))));
end

% Display results
disp('Computed shock areas (As):');
disp(Asvaluesoutletvar);

%% Theoretical Graph 1
AiAstar = tapareas./Athroat;

% Initialize results array
Msub = zeros(1, length(AiAstar));

for i = 1:length(AiAstar)
    % Define the equation as an anonymous function for each case
    Meqsubsonic = @(M) (1 ./ AiAstar(i)) .* ((1 ./ M) .* ((2 ./ (gamma+1)) .* (1 + ((gamma-1)/2) .* M.^2)) .^
((gamma+1) ./ (2*(gamma-1))))) - 1;

    % Initial guess for fsolve
    guesssubsonic = 0.5;
    % Solve for Mach number
    Msub(i) = fsolve(Meqsubsonic, guesssubsonic);
end

Msuper = zeros(1, length(AiAstar));

for i = 1:length(AiAstar)
    % Define the equation as an anonymous function for each case
    Meqsupersonic = @(M) (1 ./ AiAstar(i)) .* ((1 ./ M) .* ((2 ./ (gamma+1)) .* (1 + ((gamma-1)/2) .* M.^2)) .^
((gamma+1) ./ (2*(gamma-1))))) - 1;

    % Initial guess for fsolve
    guesssupersonic = 2;
    % Solve for Mach number
    Msuper(i) = fsolve(Meqsupersonic, guesssupersonic);
end

figure;
hold on
plot(tapposition, Msub,'r')
plot(tapposition(2:end), Msuper(2:end),'b')
xlabel('Tap Position (mm)')
ylabel('Mach Number (M)')
title('Mach Number vs Tap Position')
legend('Subsonic','Supersonic','Location','northwest')
set(gcf,'color','white')
set(gca, 'Color', 'w')

%% Theoretical Graph 2
Piposubsonic = (1 + ((gamma-1)/2).*Msub.^2).^(gamma/(gamma-1));
Piposupersonic = (1 + ((gamma-1)/2).*Msuper.^2).^(gamma/(gamma-1));
Popisubsonic = Piposubsonic.^-1;
Popisupersonic = Piposupersonic.^-1;

```

```

figure;
hold on
plot(tapposition(2:end), Popisupersonic(2:end),'r')
plot(tapposition, Popisubsonic,'b')
xlabel('Tap Position (mm)')
ylabel('P_i/P_o')
title('P_i/P_o vs Tap Position')
legend('Supersonic','Subsonic','Location','best')
set(gcf,'color','white')
set(gca, 'Color', 'w')

```

```

%% Theoretical Graph 3
Titosubsonic = (1 + ((gamma-1)/2).*Msub.^2);
Titosupersonic = (1 + ((gamma-1)/2).*Msuper.^2);
Totisubsonic = Titosubsonic.^-1;
Totisupersonic = Titosupersonic.^-1;

```

```

figure;
hold on
plot(tapposition, Totisubsonic,'r')
plot(tapposition(2:end), Totisupersonic(2:end),'b')
xlabel('Tap Position (mm)')
ylabel('T_i/T_o')
title('T_i/T_o vs Tap Position')
legend('Subsonic','Supersonic','Location','best')
set(gcf,'color','white')
set(gca, 'Color', 'w')

```

```

%% Table Values for Results
%% Table 1

```

```

%Fixed outlet pressure
varin = [100 200 300 400 450];
density1varin = [rho100inletvar(1) rho200inletvar(1) rho300inletvar(1) rho400inletvar(1) rho450inletvar(1)];
density8varin = [rho100inletvar(8) rho200inletvar(8) rho300inletvar(8) rho400inletvar(8) rho450inletvar(8)];
velocity1varin = [velocity100varin(1) velocity200varin(1) velocity300varin(1) velocity400varin(1) velocity450varin(1)];
velocity8varin = [velocity100varin(8) velocity200varin(8) velocity300varin(8) velocity400varin(8) velocity450varin(8)];
fprintf("TABLE 1\n\n")
fprintf('Fixed Outlet Pressure (50 kPa)\n\n')
for i = 1:length(varin)
    fprintf('Speed of Sound at Station 1 (%.0f): %f\n', varin(i), a1varin(i));
end
for i = 1:length(varin)
    fprintf('Density at Station 1 (%.0f): %f\n', varin(i), density1varin(i));
end
for i = 1:length(varin)
    fprintf('Velocity at Station 1 (%.0f): %f\n', varin(i), velocity1varin(i));
end
for i = 1:length(varin)
    fprintf('Speed of Sound at Station 8 (%.0f): %f\n', varin(i), a8varin(i));
end
for i = 1:length(varin)
    fprintf('Density at Station 8 (%.0f): %f\n', varin(i), density8varin(i));
end

```

```

end
for i = 1:length(varin)
    fprintf('Velocity at Station 8 (%.0f): %f\n', varin(i), velocity8varin(i));
end
%Fixed inlet pressure
varout = [50 100 200 300 400];
density1varout = [rho50outletvar(1) rho100outletvar(1) rho200outletvar(1) rho300outletvar(1) rho400outletvar(1)];
density8varout = [rho50outletvar(8) rho100outletvar(8) rho200outletvar(8) rho300outletvar(8) rho400outletvar(8)];
velocity1varout = [velocity50varout(1) velocity100varout(1) velocity200varout(1) velocity300varout(1)
velocity400varout(1)];
velocity8varout = [velocity50varout(8) velocity100varout(8) velocity200varout(8) velocity300varout(8)
velocity400varout(8) velocity50varout(8)];
fprintf('\n')
fprintf('Fixed Inlet Pressure (450 kPa)\n\n')
for i = 1:length(varout)
    fprintf('Speed of Sound at Station 1 (%.0f): %f\n', varout(i), a1varout(i));

end
for i = 1:length(varout)
    fprintf('Density at Station 1 (%.0f): %f\n', varout(i), density1varout(i));
end
for i = 1:length(varout)
    fprintf('Velocity at Station 1 (%.0f): %f\n', varout(i), velocity1varout(i));
end
for i = 1:length(varout)
    fprintf('Speed of Sound at Station 8 (%.0f): %f\n', varout(i), a8varout(i));
end
for i = 1:length(varout)
    fprintf('Density at Station 8 (%.0f): %f\n', varout(i), density8varout(i));
end
for i = 1:length(varout)
    fprintf('Velocity at Station 8 (%.0f): %f\n', varout(i), velocity8varout(i));
end

%% Table 2
inoutratiovarin = [2 4 6 8 9];
forcevarin = [Fext100varin Fext200varin Fext300varin Fext400varin Fext450varin];
fprintf('TABLE 2\n\n')
fprintf('Fixed Outlet Pressure (50 kPa)\n\n')
for i = 1:length(varout)
    fprintf('Force (Ratio is %.0f): %f\n', inoutratiovarin(i), forcevarin(i));
end
fprintf('\n')
fprintf('Fixed Inlet Pressure (450 kPa)\n\n')
inoutratiovarout = [9 4.5 2.25 1.5 1.125];
forcevarout = [Fext50varout Fext100varout Fext200varout Fext300varout Fext400varout];
for i = 1:length(varout)
    fprintf('Force (Ratio is %.0f): %f\n', inoutratiovarout(i), forcevarout(i));
end

%% Table 3
fprintf('TABLE 3\n\n')
fprintf('Fixed Outlet Pressure (50 kPa)\n\n')
percentdiffvarin = [percentdiff100varin percentdiff200varin percentdiff300varin percentdiff400varin
percentdiff450varin];

```

```

for i = 1:length(varin)
    fprintf('Percent Difference (Ratio is %.1f): %f\n', inoutratiovarin(i), percentdiffvarin(i));
end
fprintf('\n')
fprintf('Fixed Inlet Pressure (450 kPa)\n\n')
percentdiffvarout = [percentdiff50varout percentdiff100varout percentdiff200varout percentdiff300varout
percentdiff400varout];
for i = 1:length(varout)
    fprintf('Percent Difference (Ratio is %.2f): %f\n', inoutratiovarout(i), percentdiffvarout(i));
end
%% Table 4
fprintf("TABLE 4\n\n");
fprintf('Fixed Outlet Pressure (50 kPa)\n\n');
for i = 1:length(varin)
    fprintf('Shock Location Area (Ratio is %.1f): Mach number is not 1 so no shock possible\n', inoutratiovarin(i));
end
fprintf('\n');
fprintf('Fixed Inlet Pressure (450 kPa)\n\n');
for i = 1:length(varin)
    if i == 1 % Only for the first term
        fprintf('Shock Location Area (Ratio is 9.0): Mach number is not 1 so no shock possible\n');
    else
        fprintf('Shock Location Area (Ratio is %.2f): %fe-5\n', inoutratiovarout(i), Asvaluesoutletvar(i) * 10^5);
    end
end
end

```

```

%% Table Values for Appendix
%% Table A-1 Density and Uncertainty
delP = 0.1*10^3; % Taken from machine error chart (Pa)
delT = 1; % Taken from machine error chart (K)
fprintf('Varying Inlet Fixed Outlet\n')
%Density for stations 1-8 using varying inlet pressure (kg/m^3)
rho100inletvar = pi100varin.*(1000)/(R.*Tatm)
delrho100inletvar = sqrt((delP/(R*T))^2 + ((pi100varin.*(1000)/(R*T^2))*delT).^2)
rho200inletvar = pi200varin.*(1000)/(R.*Tatm)
delrho200inletvar = sqrt((delP/(R*T))^2 + ((pi200varin.*(1000)/(R*T^2))*delT).^2)
rho300inletvar = pi300varin.*(1000)/(R.*Tatm)
delrho300inletvar = sqrt((delP/(R*T))^2 + ((pi300varin.*(1000)/(R*T^2))*delT).^2)
rho400inletvar = pi400varin.*(1000)/(R.*Tatm)
delrho400inletvar = sqrt((delP/(R*T))^2 + ((pi400varin.*(1000)/(R*T^2))*delT).^2)
rho450inletvar = pi450varin.*(1000)/(R.*Tatm)
delrho450inletvar = sqrt((delP/(R*T))^2 + ((pi450varin.*(1000)/(R*T^2))*delT).^2)
fprintf('Varying Outlet Fixed Inlet\n')
rho50outletvar = pi50varout.*(1000)/(R.*Tatm);
delrho50outletvar = sqrt((delP/(R*T))^2 + ((pi50varout.*(1000)/(R*T^2))*delT).^2)
rho100outletvar = pi100varout.*(1000)/(R.*Tatm)
delrho100outletvar = sqrt((delP/(R*T))^2 + ((pi100varout.*(1000)/(R*T^2))*delT).^2)
rho200outletvar = pi200varout.*(1000)/(R.*Tatm)
delrho200outletvar = sqrt((delP/(R*T))^2 + ((pi200varout.*(1000)/(R*T^2))*delT).^2)
rho300outletvar = pi300varout.*(1000)/(R.*Tatm)
delrho300outletvar = sqrt((delP/(R*T))^2 + ((pi300varout.*(1000)/(R*T^2))*delT).^2)
rho400outletvar = pi400varout.*(1000)/(R.*Tatm)
delrho400outletvar = sqrt((delP/(R*T))^2 + ((pi400varout.*(1000)/(R*T^2))*delT).^2)

```

```
%% Table A-3 Theoretical plots data
tapposition
Msuper(1) = Msub(1);
Msupersonic = Msuper
Msubsonic = Msub
Popisupersonic(1) = Popisubsonic(1);
Popisupersonic
Popisubsonic
Totisupersonic(1) = Totisubsonic(1);
Totisupersonic
Totisubsonic
```

## Appendix D: Member Contributions

Name	Contribution
Colin McArthur	Abstract, Introduction, References, Editor
Nicolas Nelson	Appendix, Conclusion, Editor
Trae Nelson	Code, Editor
Justin Ritzenthaler	Results, Editor
Zakary Steenhoek	Procedure, Editor

## Acknowledgments

We would like to thank the AEE 362 TA's for providing us with the tools and information necessary to complete this experiment and report. We would also like to acknowledge the help that came from wonderful tools such as MATLAB and Google in providing us with resources to understand and visualize the information gathered. We also would like to thank our group members for pulling together and getting it all done on time.

## References

- [1] Anderson, John D. "Modern Compressible Flow: With Historical Perspective." 4th ed. McGraw Hill, New York, 2021. Available at: <https://platform.virdocs.com/read/1542835/215/#/4/4>. Accessed March 4, 2025.
- [2] "Compressible Flow vs. Incompressible Flow." Simscale. Last updated August 11, 2023. Available at: <https://www.simscale.com/blog/compressible-flow-vs-incompressible-flow/>. Accessed March 4, 2025.
- [3] NASA Glenn Research Center. "Choked Flow." NASA. Available at: <https://www.grc.nasa.gov/www/k-12/airplane/chokedflow.html>. Accessed March 4, 2025.
- [4] Arizona State University. "Machine Error Chart." ASU Canvas. Available at: [https://canvas.asu.edu/courses/200674/files/90846148?module\\_item\\_id=14599033](https://canvas.asu.edu/courses/200674/files/90846148?module_item_id=14599033). Accessed February 15, 2025.
- [5] MathWorks. "MATLAB 2024a." MathWorks, 2024. Available at: <https://www.mathworks.com/products/matlab.html>. Accessed February 15, 2025.
- [6] Arizona State University. "Lab 2: Experimental Investigation of Compressible Nozzle Flow." ASU Canvas. Available at: [https://canvas.asu.edu/courses/200674/files/92667506?module\\_item\\_id=14753585](https://canvas.asu.edu/courses/200674/files/92667506?module_item_id=14753585). Accessed February 13, 2025.
- [7] Arizona State University. "AEE 362 Lab 2 Data Template." Unpublished data. Available on ASU Canvas. Accessed February 15, 2024.